Open access • Journal Article • DOI:10.1109/TCPMT.2013.2259896

Variability Analysis of Interconnects Terminated by General Nonlinear Loads

Alessandro Biondi, Dries Vande Ginste, D. De Zutter, Paolo Manfredi ...+1 more authors

Institutions: Ghent University

Published on: 31 May 2013 - IEEE Transactions on Components, Packaging and Manufacturing Technology (IEEE-INST ELECTRICAL ELECTRONICS ENGINEERS INC, 445 HOES LANE, PISCATAWAY, NJ 08855 USA)

Topics: Galerkin method, Stochastic process, Nonlinear system, Time domain and Polynomial chaos

Variability Analysis of Interconnects Terminated by General Nonlinear Loads

Alessandro Biondi[1], Dries Vande Ginste[1], *Senior Member, IEEE,* Daniël De Zutter[1], *Fellow, IEEE,* Paolo Manfredi[2], *Student Member, IEEE,* Flavio Canavero[2], *Fellow, IEEE*

***Abstract*—In this paper, a stochastic modeling method is presented for the analysis of variability effects, induced by the manufacturing process, on interconnect structures terminated by general nonlinear loads. The technique is based on the solution of the pertinent stochastic Telegrapher's equations in time domain by means of the well-established stochastic Galerkin method, but now allows, for the first time in literature, the inclusion of loads with arbitrary I-V-characteristics at the terminals of the lines. The transient solution is obtained by combining the stochastic Galerkin method with a finite-difference time-domain scheme. The proposed technique is validated and illustrated with a meaningful application example, demonstrating its accuracy and efficiency.**

***Index Terms*—Multiconductor transmission line, nonlinear, stochastic Galerkin method, polynomial chaos, finite-difference time-domain, variability analysis, uncertainty**

I. Introduction

The design of electronic systems is becoming increasingly hard because of ever more stringent design specifications, expressed in terms of speed, bandwidth, crosstalk, etc. Moreover, large-scale integration and miniaturization leads to an important impact of the manufacturing process on the system performance, as this causes uncertainty of the circuit parameters. Therefore, there is a huge need for accurate and efficient stochastic modeling techniques that allow assessing the variability, induced by the manufacturing, during the early design phase [1]–[3].

On the one hand, the traditional brute-force Monte Carlo (MC) technique can be considered as a robust and reliable stochastic modeling technique. However, for complex systems, the approach is not tractable, as it is known that the convergence of the MC method is slow [4]. Improved techniques, such as quasi-MC techniques [5], have been proposed as well, but unfortunately, their applicability is limited. On the other hand, a class of so-called generalized Polynomial Chaos (gPC) techniques has been developed [6], [7] to efficiently deal with stochastic systems. These techniques turned out to be very useful for the stochastic modeling of electronic circuits and systems [8]–[12].

The authors of the present paper have especially focussed on stochastic modeling of interconnect structures that are affected by uncertainties in their geometric or material properties [13]–[15]. Thanks to the application of gPC, a modeling strategy was devised that largely outperformed traditional MC analysis. Unfortunately, as the technique developed in [13]–[15] is in essence a frequency-domain method, only linear loads, connected to the terminals of the interconnects, could be taken into account. In [10], lumped circuits with nonlinear elements were modeled as well. However, no transmission-line effects were studied, and more importantly, the nonlinearities were described by small-signal analysis or by applying a Taylor expansion around a certain bias point. Hence, all nonlinearities were of a polynomial nature, making the application of gPC again rather straightforward.

In this paper, we focus on the variability analysis of interconnects that are terminated by general nonlinear loads. The goal is to efficiently and accurately solve the governing stochastic Telegrapher's equations for multiconductor transmission lines (MTLs) and, for this purpose, the well-established Stochastic Galerkin Method (SGM) for MTLs [13]–[15] is combined with a standard finite-difference time-domain (FDTD) scheme [16]. The approach presented in this paper, however, allows for the first time in literature, and in contrast to [13]–[15], the termination of the MTLs by loads that are described by arbitrary I-V-characteristics. It will be shown that these I-V-characteristics can be of a very general nature, even non-smooth, non-polynomial functions can be dealt with. Via numerical integration, an FDTD-update scheme is obtained that requires the solution of a set of nonlinear equations, which can be solved efficiently by providing it with a clever and convenient choice of a seed.

This paper is organized as follows. In Section II, the proposed formalism is explained starting from the stochastic Telegrapher's equations. The SGM framework is constructed and special attention is devoted to the description of nonlinear loads and to their FDTD implementation. In Section III, the formalism is validated and illustrated by applying it to the variability analysis of a pair of coupled microstrip lines, terminated by a diode, described by a nonlinear, non-smooth I-V-characteristic. Conclusions are summarized in Section IV.

II. Stochastic Modeling Formalism and Implementation

A. Stochastic Telegrapher's Equations

Consider a uniform multiconductor transmission line (MTL) where the axis of invariance is the z-axis. In general, the MTL consists of $\mathcal{N}$ signal conductors and a reference conductor. An example of such a line is given in Fig. 1 (Section III), where $\mathcal{N} = 2$. An MTL's behavior is described by the well-known

[1] Electromagnetics Group, Department of Information Technology, Ghent University, Sint-Pietersnieuwstraat 41, 9000 B-Gent, Belgium. E-mail: alessandro.biondi@UGent.be, Tel.: +32 9 264 35 93, Fax: +32 9 264 99 69.

[2] EMC Group, Dipartimento di Elettronica, Politecnico di Torino, Corso Duca degli Abruzzi 24, 10129 Torino, Italy.

Telegrapher's equations [17]. Often, due to manufacturing, one or more geometrical and/or material parameters are not known in a deterministic way. They have to be treated as stochastic random variables (RVs), characterized by a probability density function (PDF), rendering the Telegrapher's equations nondeterministic. For ease of notation, but without loss of generality, in this section, we consider a single lossless dispersion-free line ($\mathcal{N} = 1$), affected by a single stochastic parameter. (In Section III, an example is given for $\mathcal{N} = 2$ and two stochastic parameters.) We can then write the pertinent *stochastic* Telegrapher's equations as follows:

$$\frac{\partial}{\partial z}\begin{bmatrix} v(z,t,\beta) \\ i(z,t,\beta) \end{bmatrix} = -\begin{bmatrix} 0 & L(\beta) \\ C(\beta) & 0 \end{bmatrix} \cdot \frac{\partial}{\partial t}\begin{bmatrix} v(z,t,\beta) \\ i(z,t,\beta) \end{bmatrix}, \tag{1}$$

where v and i are the voltage and current along the line, and with L and C the per-unit-of-length (p.u.l.) transmission line parameters, i.e. the p.u.l. inductance and capacitance respectively. Next to the position z along the line and the time t, we have also explicitly written down the dependence on a stochastic parameter β, of which only the PDF is known, prohibiting a straightforward solution of (1). From here on, we denote this PDF of β by $W_\beta(\beta)$, which is defined on a support $\Gamma \subseteq \mathbb{R}$.

B. Stochastic Galerkin Method (SGM)

To solve the stochastic Telegrapher's equations (1), we rely on the so-called Stochastic Galerkin Method (SGM). For a detailed description of this method, applied to transmission lines in the frequency domain, we refer to [13]–[15]. Here, we repeat the gist of it in the time domain. This will allow us to demonstrate in Section II-C how the method can be adapted and leveraged to include general nonlinear terminations.

The first step of the SGM is to apply a Polynomial Chaos (PC) expansion, by rewriting the voltage, current and p.u.l. parameters as follows:

$$\begin{aligned} v(z,t,\beta) &= \sum_{k=0}^{K} v_k(z,t)\phi_k(\beta), \quad L(\beta) = \sum_{k=0}^{K} L_k\phi_k(\beta), \\ i(z,t,\beta) &= \sum_{k=0}^{K} i_k(z,t)\phi_k(\beta), \quad C(\beta) = \sum_{k=0}^{K} C_k\phi_k(\beta), \end{aligned} \tag{2}$$

where each function $\phi_k(\beta)$, $k = 0,\ldots,K$, represents a polynomial of degree k. For an efficient expansion, leading to an adequate solution of the stochastic Telegrapher's equations, these polynomials are chosen according to the Wiener-Askey scheme [18], meaning that they are orthogonal w.r.t. to the following inner product:

$$<\phi_k(\beta),\phi_l(\beta)> = \int_\Gamma \phi_k(\beta)\,\phi_l(\beta)\,W_\beta(\beta)\,d\beta = c_k\delta_{kl}. \tag{3}$$

In the above equation (3), the weighting function $W_\beta(\beta)$ coincides with the PDF of β, and δ_{kl} is the Kronecker delta. The scalar number c_k simply depends on the scaling of the polynomials, e.g., if the polynomials are chosen to be ortho*normal*, then $c_k = 1$, $\forall k = 0,\ldots,K$ [19]. Thanks to the orthogonality, upon knowledge of the p.u.l. parameters L and C as a function of β, the expansion coefficients L_k and C_k, $k = 0,\ldots,K$, are readily computed. The voltage and current expansion coefficients, i.e. v_k and i_k resp., $k = 0,\ldots,K$, are yet unknown.

In the second step of the SGM, the expansions (2) are substituted into (1) and the result is subjected to a Galerkin testing procedure [20], meaning that the equations are weighted with the same set of polynomials using the inner product (3). This leads to the following set of equations:

$$\frac{\partial}{\partial z}\begin{bmatrix} \tilde{\mathbf{v}}(z,t) \\ \tilde{\mathbf{i}}(z,t) \end{bmatrix} = -\begin{bmatrix} 0 & \tilde{\overline{\mathbf{L}}} \\ \tilde{\overline{\mathbf{C}}} & 0 \end{bmatrix} \cdot \frac{\partial}{\partial t}\begin{bmatrix} \tilde{\mathbf{v}}(z,t) \\ \tilde{\mathbf{i}}(z,t) \end{bmatrix}, \tag{4}$$

where $\tilde{\mathbf{v}}$ and $\tilde{\mathbf{i}}$ are $(K+1)$-vectors containing the voltage and current expansion coefficients v_k and i_k, and where $\tilde{\overline{\mathbf{L}}}$ and $\tilde{\overline{\mathbf{C}}}$ are $(K+1)\times(K+1)$ matrices, with matrix elements $\tilde{L}_{ml} = \sum_{k=0}^{K} L_k\alpha_{klm}$ and $\tilde{C}_{ml} = \sum_{k=0}^{K} C_k\alpha_{klm}$ where $\alpha_{klm} = <\phi_k(\beta)\phi_l(\beta),\phi_m(\beta)>/c_m$ $(l,m = 0,\ldots,K)$. In summary, thanks to the SGM, we have gone from a set of two stochastic equations (1) to an augmented set of $2(K+1)$ deterministic equations (4). Indeed, in (4), the dependency on β has vanished at the cost of an increased number of unknowns, being the voltage and currents expansion coefficients v_k and i_k. Additionally, it is worth mentioning that the augmented equations (4) have exactly the same shape as a classical set of Telegrapher's equations for $K+1$ lines, and it has been proven in [19] and [21] that reciprocity and passivity of these "augmented lines" are preserved.

C. Boundary Conditions (BCs): General Nonlinear Loads

From the above, it can be concluded that upon knowledge of the $2(K+1)$ unknown expansion coefficients v_k and i_k, $k = 0,\ldots,K$, the stochastic problem is fully determined. To find these unknowns, the set of $2(K+1)$ augmented equations (4) needs to be solved using standard mathematical methods, and hence, a proper set of $2(K+1)$ boundary conditions (BCs) is required. These BCs evolve from the generators and loads attached to the terminals of the original stochastic line (1). It has been explained in [15] that linear loads can easily be dealt with. In this paper, however, we focus on the inclusion of general nonlinear loads, described by arbitrary I-V-characteristics, within the well-established SGM framework. This opens up a much wider range of applications.

Consider again the single stochastic line, described by (1), with a finite length $\mathcal{L}$. We assume that a nonlinear load is attached to the far-end terminal, i.e. at $z = \mathcal{L}$:

$$i(\mathcal{L},t,\beta) = F(v(\mathcal{L},t,\beta)), \tag{5}$$

where $F(\cdot)$ represents a general nonlinear function. To construct the pertinent BCs, allowing to solve the augmented equations (4), we proceed as follows. First, the PC-expansions (2) of the voltage and the current at the load are inserted into (5):

$$\sum_{k=0}^{K} i_k(\mathcal{L},t)\phi_k(\beta) = F\left(\sum_{k=0}^{K} v_k(\mathcal{L},t)\phi_k(\beta)\right). \tag{6}$$

Second, (6) is Galerkin tested, yielding:

$$\forall m = 0, \ldots, K:$$
$$i_m(\mathcal{L},t) = \frac{1}{c_m} < F\left(\sum_{k=0}^{K} v_k(\mathcal{L},t)\phi_k(\beta)\right), \phi_m(\beta) > . \quad (7)$$

Note that for linear loads [15] and for loads described by a polynomial function $F(\cdot)$ [10], the inner product in the rhs of (7) can be calculated analytically, leading to a simple set of $(K+1)$ BCs for the equations (4). Such a set of augmented BCs represents a linear or polynomial relationship between the voltage and current expansion coefficients at the terminal $z = \mathcal{L}$. In contrast, for arbitrary, nonlinear $F(\cdot)$, such an approach is not possible, and therefore, we will now construct an approximate analytical relationship between the current and voltage expansion coefficients at the terminals. Thereto, the integral pertaining to the inner product, is solved numerically, as follows:

$$\begin{aligned} &< F\left(\sum_{k=0}^{K} v_k(\mathcal{L},t)\phi_k(\beta)\right), \phi_m(\beta) > \\ &= \int_\Gamma F\left(\sum_{k=0}^{K} v_k(\mathcal{L},t)\phi_k(\beta)\right) \phi_m(\beta)\, W_\beta(\beta)\, d\beta \\ &\approx \sum_{n=1}^{N} w_n\, G_{n,m}(v_0(\mathcal{L},t), \ldots, v_K(\mathcal{L},t), \beta_n), \end{aligned} \quad (8)$$

with

$$\begin{aligned} &G_{n,m}(v_0(\mathcal{L},t), \ldots, v_K(\mathcal{L},t), \beta_n) \\ &\quad = F\left(\sum_{k=0}^{K} v_k(\mathcal{L},t)\phi_k(\beta_n)\right) \phi_m(\beta_n). \end{aligned} \quad (9)$$

In (8), any kind of numerical integration technique can be used, ranging from the classical trapezoidal rule, over Gaussian quadrature rules, to highly adaptive integration schemes [22]. In all these cases, and depending on the desired accuracy, the integration comes down to selecting N nodes β_n in the domain Γ and a corresponding set of N weights w_n. (Obviously, it is hard to exactly predict the number of nodes that is strictly required for all kinds of nonlinearities that one can encounter. Nonetheless, an illustrative example is given in Section III.) Finally, a set of $(K+1)$ BCs is found, being a set of $K+1$ coupled, nonlinear relations between the voltage and current expansion coefficients at the terminals $z = \mathcal{L}$ of the augmented lines (4), as follows:

$$\forall m = 0, \ldots, K:\ i_m(\mathcal{L},t) \approx \tilde{F}_m(v_0(\mathcal{L},t), \ldots, v_K(\mathcal{L},t)), \quad (10)$$

or in vector form

$$\tilde{\mathbf{i}}(\mathcal{L},t) \approx \tilde{\mathbf{F}}\left[\tilde{\mathbf{v}}(\mathcal{L},t)\right], \quad (11)$$

where, after omitting the argument, the nonlinear functions $\tilde{F}_m$, $m = 0, \ldots, K$, contained in the vector of functions $\tilde{\mathbf{F}}$, are given by

$$\tilde{F}_m = \frac{1}{c_m} \sum_{n=1}^{N} w_n\, G_{n,m}. \quad (12)$$

Note that in the above expressions the $\approx$-sign was used explicitly to stress that no analytically correct calculation can be obtained, this in contrast to the case where linear or polynomial loads are used. Nevertheless, still a very good accuracy is obtained, as shown in Section III. Obviously, a similar technique can be used at the other terminal $z = 0$, leading to a second set of $K+1$ BCs, allowing to solve the $2(K+1)$ equations (4).

D. Implementation via the Finite-Difference Time-Domain (FDTD) Method

To solve the augmented set of equations (4) in conjunction with a set of nonlinear BCs such as (11), in this paper we adopt a finite-difference time-domain (FDTD) technique for transmission lines [17]. Of course, as the above formulation to handle nonlinearities is in fact independent from the time-domain solution technique, other methods, such as, e.g., waveform relaxation techniques [23] could be used as well. We now briefly recapitulate the FDTD method for transmission lines. We opt not to dwell on the inclusion of frequency-dependent losses, but rather focus on the implementation of the nonlinear terminations (11). For a detailed explanation on FDTD we refer the reader to [16], [17].

The line of length $\mathcal{L}$ is divided into N_z equal sections of length Δz. In a similar fashion, the total simulation time is divided into N_t time segments of length Δt. The voltage waveforms $v_k(z,t)$ along the line are assessed in N_z+1 discrete nodes $z_p = p\Delta z$, $p = 0, \ldots, N_z$, and at times $q\Delta t$, $q = 0, \ldots, N_t$. The current waveforms $i_k(z,t)$ are assessed in N_z discrete nodes $z_p = (p+\frac{1}{2})\Delta z$, $p = 0, \ldots, N_z-1$, and at times $(q+\frac{1}{2})\Delta t$, $q = 0, \ldots, N_t-1$. This interlacing guarantees an accurate FDTD-scheme. The voltage and current variables, discretized in space and time according to this scheme, are contained in $(K+1)$-vectors $\tilde{\mathbf{v}}_p^q$ and $\tilde{\mathbf{i}}_{p+\frac{1}{2}}^{q+\frac{1}{2}}$. After discretization of the Telegrapher's equations (4), i.e. after approximating the derivatives $\frac{\partial}{\partial z}$ and $\frac{\partial}{\partial t}$ by finite differences and neglecting second-order terms, the following typical FDTD-leapfrog scheme is obtained:

$$\tilde{\mathbf{v}}_p^{q+1} = \tilde{\mathbf{v}}_p^q - \frac{\Delta t}{\Delta z}\tilde{\overline{\mathbf{C}}}^{-1} \cdot \left(\tilde{\mathbf{i}}_{p+\frac{1}{2}}^{q+\frac{1}{2}} - \tilde{\mathbf{i}}_{p-\frac{1}{2}}^{q+\frac{1}{2}}\right), \quad (13)$$

$$\tilde{\mathbf{i}}_{p+\frac{1}{2}}^{q+\frac{3}{2}} = \tilde{\mathbf{i}}_{p+\frac{1}{2}}^{q+\frac{1}{2}} - \frac{\Delta t}{\Delta z}\tilde{\overline{\mathbf{L}}}^{-1} \cdot \left(\tilde{\mathbf{v}}_{p+1}^{q+1} - \tilde{\mathbf{v}}_p^{q+1}\right). \quad (14)$$

The voltages and currents are solved by iterating p for a fixed time (recursively solving first (13) and second (14)), and then iterating time. All voltage and current variables are treated in this way, except for the voltages at the terminals $z = 0$ ($p = 0$) and $z = \mathcal{L}$ ($p = N_z$), for which special update functions need to be constructed. It is readily proven [17] that these are given by:

$$\tilde{\mathbf{v}}_0^{q+1} = \tilde{\mathbf{v}}_0^q - \frac{2\Delta t}{\Delta z}\tilde{\overline{\mathbf{C}}}^{-1} \cdot \left(\tilde{\mathbf{i}}_0^{q+\frac{1}{2}} - \tilde{\mathbf{i}}_{\mathrm{ne}}^{q+\frac{1}{2}}\right), \quad (15)$$

$$\tilde{\mathbf{v}}_{N_z}^{q+1} = \tilde{\mathbf{v}}_{N_z}^q - \frac{2\Delta t}{\Delta z}\tilde{\overline{\mathbf{C}}}^{-1} \cdot \left(\tilde{\mathbf{i}}_{\mathrm{fe}}^{q+\frac{1}{2}} - \tilde{\mathbf{i}}_{N_z-1}^{q+\frac{1}{2}}\right), \quad (16)$$

where the vectors $\tilde{\mathbf{i}}_{\mathrm{ne}}^{q+\frac{1}{2}}$ and $\tilde{\mathbf{i}}_{\mathrm{fe}}^{q+\frac{1}{2}}$ contain the $(K+1)$ currents flowing through the terminals at the near-end $z = 0$ and the far-end $z = \mathcal{L}$ respectively. Consider now nonlinear

loads at the far-end, described by general nonlinear I-V-characteristics (11), here repeated in discretized form:

$$\tilde{\mathbf{i}}_{\mathrm{fe}}^{q+\frac{1}{2}} \approx \tilde{\mathbf{F}}\left[\tilde{\mathbf{v}}_{N_z}^{q+\frac{1}{2}}\right] \approx \tilde{\mathbf{F}}\left[\frac{1}{2}\left(\tilde{\mathbf{v}}_{N_z}^{q} + \tilde{\mathbf{v}}_{N_z}^{q+1}\right)\right]. \qquad (17)$$

To update the value of the voltage variables at the terminal, (17) is inserted into (16) as follows,

$$\tilde{\mathbf{v}}_{N_z}^{q+1} = \tilde{\mathbf{v}}_{N_z}^{q} - \frac{2\Delta t}{\Delta z}\tilde{\overline{\mathbf{C}}}^{-1}\cdot\left(\tilde{\mathbf{F}}\left[\frac{1}{2}\left(\tilde{\mathbf{v}}_{N_z}^{q} + \tilde{\mathbf{v}}_{N_z}^{q+1}\right)\right] - \tilde{\mathbf{i}}_{N_z-1}^{q+\frac{1}{2}}\right), \qquad (18)$$

and this equation should be solved for $\tilde{\mathbf{v}}_{N_z}^{q+1}$. At the near-end $z = 0$, a similar procedure can be applied, solving for $\tilde{\mathbf{v}}_{0}^{q+1}$. For general nonlinear functions $\tilde{\mathbf{F}}[\cdot]$, often, (18) is a transcendental equation. In our work, the FDTD scheme is implemented in Matlab, and the update function (18) is handled by making use of the `fsolve.m` routine, which allows to find the roots of a set of coupled nonlinear equations. It is interesting to mention that, thanks to the FDTD scheme, we can assure a fast converge of the iterative solution provided by this `fsolve`-routine. Indeed, to find the update value for $\tilde{\mathbf{v}}_{N_z}^{q+1}$, we seed the solver with the previous voltage $\tilde{\mathbf{v}}_{N_z}^{q}$, which turns out to be an excellent initial value. The discretization step Δz is chosen sufficiently small to properly resolve all wave dynamics. By respecting the Courant condition $\Delta t \leq \frac{\Delta z}{v_{\max}}$, with $v_{\max}$ the speed of the fastest fundamental eigenmode pertaining to the $K+1$ lines, the actual waveform can be reproduced with very good accuracy.

III. Numerical Results

In this section, the above outlined technique is validated and illustrated by applying it to the variability analysis of a pair of coupled PEC microstrip lines ($\mathcal{N} = 2$). The cross-section of the lines is given in Fig. 1(a), where $w = 100$ μm, $h = 500$ μm and $t = 35$ μm. The gap G between the lines and the relative permittivity ϵ_r of the substrate are considered to be two Gaussian RVs with means $\mu_G = 80$ μm and $\mu_{\epsilon_r} = 4$ respectively, and with normalized standard deviations $\sigma_G = 5\%$ and $\sigma_{\epsilon_r} = 5\%$. As shown in Fig. 1(b), the lines are given a length of $\mathcal{L} = 5$ cm. One line, called the active line, is excited by means of a voltage source $v_s(t)$ that produces a ramped step, going from 0 V to 1 V in a risetime of 100 ps. The generator impedance is $R_{g1} = 50\ \Omega$. This active line is terminated by means of a forward biased diode. The diode's I-V-characteristic is given by:

$$i = F(v) = \begin{cases} 0 & , v < v_1 \\ \frac{v-v_1}{R_1} & , v_1 \leq v < v_2 \\ \frac{v-v_2}{R_2} + \frac{v_2-v_1}{R_1} & , v \geq v_2 \end{cases}, \qquad (19)$$

where $v_1 = 0.67$ V, $v_2 = 0.73$, $R_1 = 1\ \Omega$, and $R_2 = 0.1\ \Omega$. This is a three-line piecewise linear model [24], as shown in Fig. 2. This kind of model is chosen for three reasons. First, such a model is often preferred because of the presence of the current-limiting resistor R_2, this in contrast to the well-known Shockley-model $i = I_s\left(e^{\frac{v}{\eta V_t}} - 1\right)$ with an exponentially increasing current. Second, it allows to show that even non-smooth, complex I-V-characteristics can be treated with great accuracy and efficiency with our technique, which is rather challenging. (For comparison, the smooth Shockley model's I-V-characteristic is also shown on Fig. 2, where the typical parameters are $I_s = 5 \cdot 10^{-14}$ A, $\eta = 1$, and $V_t = 25.85$ mV.) Third, the nonlinearity induced by this I-V-characteristic will lead to a clipping of the voltage across the load. Hence, this can be considered as a "hard nonlinearity", in contrast to, e.g., the rather mild distortion introduced by amplifiers working in small-signal regime or by I/O buffers with a very high input impedance. The second line, called the victim line, is terminated at the near-end by means of a 50 Ω load R_{g2}. At the far-end, a 1 pF ideal capacitor C_L is connected. We are interested in the voltage waveforms v_{in} at the input of the active line, v_{out} at the diode, the near-end crosstalk v_{NX} and the far-end crosstalk v_{FX}, all indicated on Fig. 1.

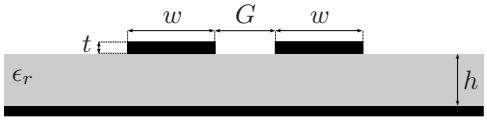

(a) Cross-section AA' of the source-line-load configuration (Fig. 1(b)), where $w = 100$ μm, $h = 500$ μm and $t = 35$ μm. The gap G between the lines and the relative permittivity ϵ_r of the substrate are stochastic parameters.

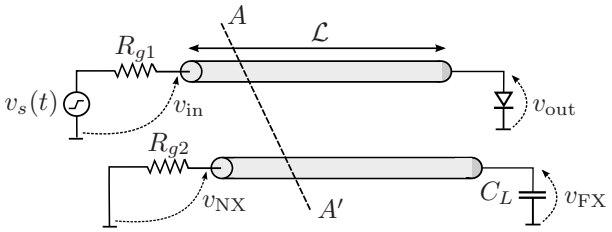

(b) Source-line-load configuration, using cross-section AA' (Fig. 1(a)), where $\mathcal{L} = 5$ cm, $v_s(t)$ is a ramped voltage step, $R_{g1} = R_{g2} = 50\ \Omega$, $C_L = 1$ pF, and the diode's I-V-characteristic is given by (19).

Fig. 1: Pair of coupled microstrip lines under study.

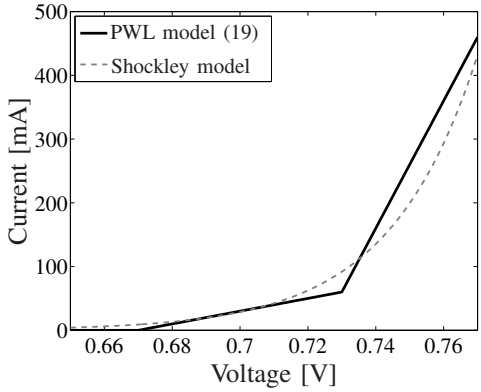

Fig. 2: Three-line piecewise linear (PWL) diode model according to (19). (For comparison, the Shockley model $i = I_s\left(e^{\frac{v}{\eta V_t}} - 1\right)$, with $I_s = 5 \cdot 10^{-14}$ A, $\eta = 1$, and $V_t = 25.85$ mV, is plotted as well.)

To obtain a reference result, first, a Monte Carlo (MC) simulation was performed using 10000 samples of G and ϵ_r, drawn according to their respective Gaussian distribution.

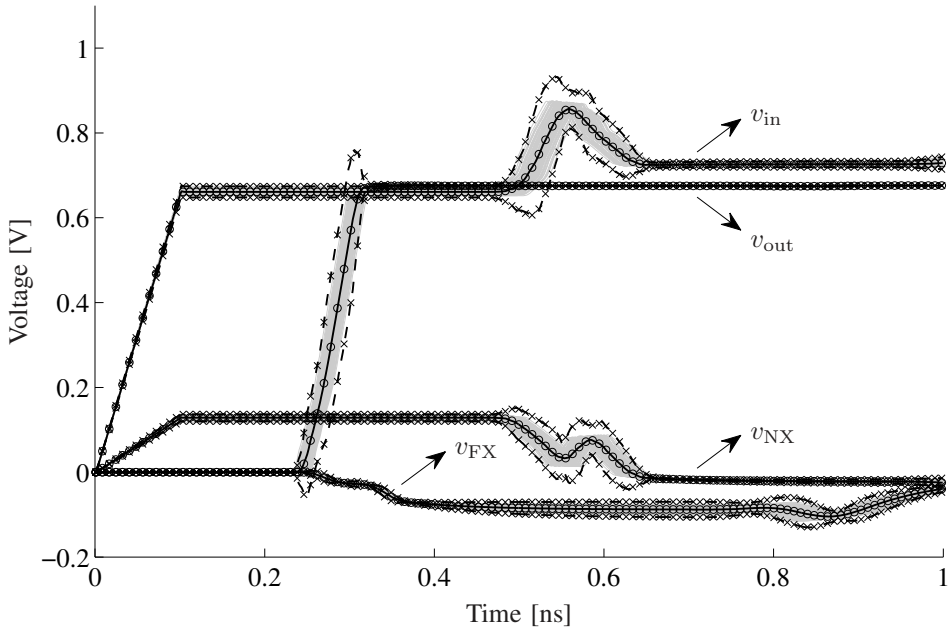

Fig. 3: Voltage waveforms $v_{\rm in}(t)$, $v_{\rm out}(t)$, $v_{\rm NX}(t)$, and $v_{\rm FX}(t)$, at the four terminals of the coupled microstrip lines of Fig. 1. Full black lines: means μ_v computed using the SGM-FDTD technique; Dashed black line: $\pm 3\sigma_v$-variations computed using the SGM-FDTD technique; Circles ($\circ$): means μ_v computed using the MC technique; Crosses ($\times$): $\pm 3\sigma_v$-variations computed using the MC technique; Gray lines: 100 MC samples.

These 10000 FDTD simulations were performed using the following settings: $\Delta_t = 0.792$ ps and $\Delta_z = 0.192$ mm. Next, the proposed SGM for nonlinear loads was used. A set of $K+1 = 10$ orthonormal Hermite polynomials [18] was adopted to model the variability and the numerical integration was performed using 100 cubature points. The FDTD settings were the following: $\Delta_t = 0.842$ ps and $\Delta_z = 0.198$ mm. These SGM-FDTD settings differ slightly from the MC-FDTD settings, because with SGM, actually, an augmented set of $\mathcal{N}(K+1) = 20$ lines was modeled. This augmented MTL clearly exhibits a different eigenmode behavior than the original set of two lines, used during the MC run, hence a different discretization is needed. In Fig. 3 the result is presented. The full black lines indicate the means μ_v of the four voltage waveforms $v_{\rm in}(t)$, $v_{\rm out}(t)$, $v_{\rm NX}(t)$, and $v_{\rm FX}(t)$, at the four terminals of the coupled microstrip lines of Fig. 1, and the dashed lines show the $\pm 3\sigma_v$ deviations from these means μ_v, all computed using the SGM-FDTD technique. Thanks to the gPC-representation, the mean and standard deviation of a voltage waveform $v(z,t,G,\epsilon_r)$ are very efficiently calculated as follows [7]:

$$\mu_{v(z,t,G,\epsilon_r)} = v_0(z,t), \tag{20}$$

$$\sigma_{v(z,t,G,\epsilon_r)} = \sqrt{\sum_{k=1}^{K} (v_k(z,t))^2}, \tag{21}$$

where v_k, $k = 0,\ldots,K$, are the voltage expansion coefficients, obtained by means of the SGM-FDTD. The gray lines on Fig. 3 correspond to 100 samples of the MC run; the circles ($\circ$) and crosses ($\times$) indicate the mean μ_v and the $\pm 3\sigma_v$ deviations, resp., computed using the 10000 samples of the MC run. Apart from the hard nonlinearity induced by the diode, an excellent correspondence between the SGM results and the MC results is observed. Moreover, such graphs can be computed in a very efficient way now. Indeed, whereas he total run time for this MC analysis was 53582 s, the SGM simulation only took 75 s. So, an impressive speed-up factor of 714 is obtained by means of the newly proposed technique. All computations have been performed on a Dell Precision M4500 laptop with an Intel(R) Core(TM) i7 X940 CPU running at 2.13 GHz and 8 GB of RAM.

At this point, it is instructive to comment on the convergence of the MC method. One might argue that 10000 samples seems a lot for this kind of example, but in fact, it is not. In Fig. 4 the relative error on the computed mean and variance of the maximum of the far-end crosstalk $\max_{t\geq 0}|v_{\rm FX}(t)|$ is shown as a function of $N_{\rm MC}$, i.e. the number of MC samples used. The mean and variance of $\max_{t\geq 0}|v_{\rm FX}(t)|$, obtained by using all 10000 samples, are 0.10759 V and $1.2552\cdot 10^{-5}$ V^2 respectively. These values are used as the reference result to compute the relative errors, shown in Fig. 4. As expected, a $1/\sqrt{N_{\rm MC}}$-convergence rate is obtained. It is also observed that although using 1000 or 2000 samples might be sufficient to obtain a good estimate of the mean, it is not sufficient to get a an accurate result for the variance. The relative error just drops below 1% when 10000 samples are used. In the signal integrity applications we have in mind, it is not sufficient to know the mean value of the crosstalk. Typically, one is interested in the maximum value. To obtain higher-order stochastic moments with sufficient accuracy or to reconstruct the cumulative distribution function (see below), a large number of MC samples is needed. In this perspective,

the speed-up factor presented above is not exaggerated and it is safe to state that also for larger examples (with more RVs), still a considerable speed-up w.r.t. MC simulations will be obtained.

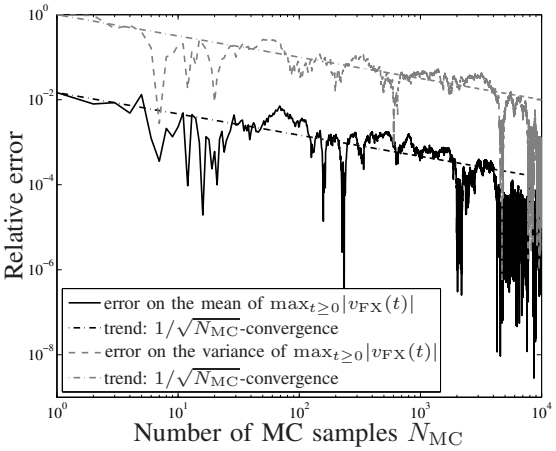

Fig. 4: Convergence of the MC simulation: relative error on the computed mean and variance of the maximum far-end crosstalk, as a function of the number of MC samples used.

As stated above, a designer is typically interested in the maximum amount of crosstalk he/she can expect. Therefore, in a post-processing step, we compute the cumulative distribution function (CDF) of the maximum of the near-end and far-end crosstalk, i.e. we compute the CDFs of $\max_{t\geq 0}|v_{\mathrm{NX}}(t)|$ and $\max_{t\geq 0}|v_{\mathrm{FX}}(t)|$, using standard analytical or numerical techniques [25]. The results are shown in Figs. 5 and 6. Although the number of MC samples was still not extremely high, again a good agreement between MC and the SGM-FDTD technique is obtained. From these figures, it is easy to estimate the maximum crosstalk levels that one can expect, or alternatively, it is now readily seen that, e.g., there is an 80% chance that the crosstalk will take a value less than or equal to 131 mV at the near-end terminal and 110 mV at the far-end terminal.

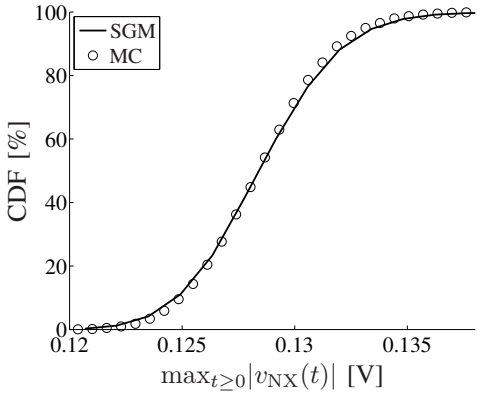

Fig. 5: Cumulative distribution function (CDF) of the maximum of the near-end crosstalk as presented in Fig. 3.

To obtain the above results, we opted to use a Gauss-Hermite cubature integration scheme [26] to compute the inner products (8). This is a logical choice for this integral, since

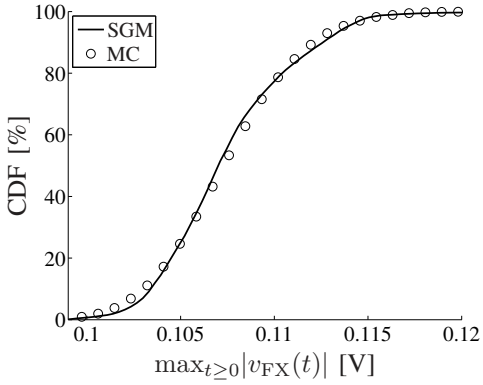

Fig. 6: Cumulative distribution function (CDF) of the maximum of the far-end crosstalk as presented in Fig. 3.

the weighting function in the integrand represents a probability density function pertaining to the two independent Gaussian RVs G and ϵ_r. The influence of the number of cubature points, used in the two-dimensional domain Γ, is indicated in Table I. In this table, we present the mean and the variance of $\max_{t\geq 0}|v_{\mathrm{FX}}(t)|$, computed by the 10000 MC samples on the one hand and by the SGM-FDTD method on the other. When the number of cubature points increases to about 10×10, the relative error of SGM-FDTD, compared to MC, drops to the levels that we can expect from Fig. 4, i.e. two digits of accuracy on the variance and four digits of accuracy on the mean. All results presented above were obtained with this 10×10 cubature scheme.

Technique	$\max_{t\geq 0}\lvert v_{\mathrm{FX}}(t)\rvert$		Relative error [%]	
(# cubature points)	mean [V]	variance [V^2]	mean	variance
MC (10^4 samples)	0.10759	$1.2552{\cdot}10^{-5}$	0	0
SGM (1×1)	0.13496	$1.8519{\cdot}10^{-2}$	25.4	$> 10^6$
SGM (2×2)	0.10853	$6.5588{\cdot}10^{-5}$	0.871	423
SGM (5×5)	0.10764	$1.3088{\cdot}10^{-5}$	0.0438	4.27
SGM (10×10)	0.10761	$1.2473{\cdot}10^{-5}$	0.0179	0.634

TABLE I: Influence of the number of cubature points (indicated between brackets) in the two-dimensional domain Γ, used in the computation of the inner products (8), on the mean and the variance of the maximum of the far-end crosstalk. The relative accuracy w.r.t. the MC run with 10000 samples is also indicated.

IV. Conclusions

Due to very stringent design specifications, the design of interconnects has become a challenging task. Moreover, the manufacturing process causes geometrical and material parameter uncertainties, necessitating the development of stochastic modeling tools that allow assessing the variability effects. In recent literature, polynomial chaos (PC) based techniques have been developed for lumped circuits and distributed interconnects, proving their ability for accurate and efficient variability analysis. However, so far, stochastic interconnect structures could only be terminated by linear loads and PC-based techniques for stochastic lumped circuits could only take mild nonlinearities, described by polynomial I-V-characteristics, into account. Therefore, in this paper, we

solve the stochastic Telegrapher's equations for multiconductor transmission lines (MTLs), by combining the well-established stochastic Galerkin method (SGM) with a finite-difference time-domain (FDTD) scheme. The novelty of this paper lies in the fact that the SGM-FDTD framework is adapted and leveraged for the first time to also include general nonlinear loads, described by arbitrary I-V-characteristics, at the terminals of the MTL. This opens up a much wider range of applications that can now be tackled. The technique was validated and illustrated by means of an application example, consisting of a pair of coupled microstrip lines exhibiting variability of its geometrical and material parameters, and terminated by a diode with a non-smooth I-V-characteristic. Compared to a standard, robust Monte Carlo analysis, the method shows excellent agreement and far superior efficiency.

Future research, as also pointed out by the reviewers, will focus on the inclusion of (behavioral models of) *dynamic* nonlinear terminations [27], as well as on the extension of the application examples to I/O bus structures with many random variables. With respect to the latter extension, the scalability of the SGM becomes an important issue. This has also already been adressed in [13], [14]. Also, a comparison with a non-intrusive stochastic modeling technique, such as the stochastic collocation method (SCM) [28], might be useful, as the SCM is more parallelizable than the SGM.

REFERENCES

[1] T. Mikazuki and N. Matsui, "Statistical design techniques for high-speed circuit boards with correlated distributions," *IEEE Trans. Comp. Pack. & Man. Tech. Part A*, vol. 17, no. 1, pp. 159–165, Mar. 1994.

[2] A. H. Zaabab, Q.-J. Zhang, and M. Nakhla, "A neural network modeling approach to circuit optimization and statistical design," *IEEE Trans. Microw. Theory Tech.*, vol. 43, no. 6, pp. 1349–1358, Jun. 1995.

[3] Q. Zhang, J. J. Liou, J. McMacken, J. Thomson, and P. Layman, "Development of robust interconnect model based on design of experiments and multiobjective optimization," *IEEE Trans. Electron Devices*, vol. 48, no. 9, pp. 1885–1891, Sep. 2001.

[4] G. S. Fishman, *Monte Carlo: Concepts, Algorithms, and Applications*. New York: Springer-Verlag, 1996.

[5] H. Niederreiter, P. Hellekalek, G. Larcher, and P. Zinterhof, *Monte Carlo and Quasi-Monte Carlo Methods*. New York: Springer-Verlag, 1998.

[6] R. G. Ghanen and P. D. Spanos, *Stochastic Finite Elements. A Spectral Approach*. New York, USA: Springer-Verlag, 1991.

[7] D. Xiu, "Fast numerical methods for stochastic computations: A review," *Communications in Computational Physics*, vol. 5, no. 2-4, pp. 242–272, Feb. 2009.

[8] Q. Su and K. Strunz, "Stochastic circuit modelling with Hermite polynomial chaos," *Electronic Letters*, vol. 41, no. 21, pp. 1163–1165, Oct. 2005.

[9] S. Vrudhula and J. M. W. P. Ghanta, "Hermite polynomial based interconnect analysis in the presence of process variations," *IEEE Trans. Comput. Aided Design Int. Circ. Syst.*, vol. 25, no. 10, pp. 2001–2011, Oct. 2006.

[10] K. Strunz and Q. Su, "Stochastic formulation of SPICE-type electronic circuit simulation with polynomial chaos," *ACM Trans. on Modeling and Computer Simulation*, vol. 18, no. 4, pp. 15:1–15:23, Sep. 2008.

[11] P. Sumant, H. Wu, A. Cangellaris, and N. Aluru, "Reduced-order models of finite elements approximations of electromagnetic devices exhibiting statistical variability," *IEEE Trans. Antennas Propag.*, vol. 60, no. 1, pp. 301–309, Jan. 2012.

[12] D. Spina, F. Ferranti, T. Dhaene, L. Kockaert, G. Antonini, and D. Vande Ginste, "Variability analysis of multiport systems via polynomial-chaos expansion," *IEEE Trans. Microw. Theory Tech.*, vol. 60, no. 8, pp. 2329–2338, Aug. 2012.

[13] I. S. Stievano, P. Manfredi, and F. G. Canavero, "Stochastic analysis of multiconductor cables and interconnects," *IEEE Trans. Electromagn. Compat.*, vol. 53, no. 2, pp. 501–507, May 2011.

[14] ——, "Parameters variability effects on multiconductor interconnects via Hermite polynomial chaos," *IEEE Trans. on Components, Packaging and Manufacturing Technology*, vol. 1, no. 8, pp. 1234–1239, Aug. 2011.

[15] D. Vande Ginste, D. De Zutter, D. Deschrijver, T. Dhaene, P. Manfredi, and F. Canavero, "Stochastic modeling based variability analysis of on-chip interconnects," *IEEE Transactions on Components, Packaging and Manufacturing Technology*, vol. 2, no. 7, pp. 1182–1192, Jul. 2012.

[16] A. Taflove, *The Finite-Difference Time Domain Method*. Norwood: Artech House, 1995.

[17] C. R. Paul, *Analysis of Multiconductor Transmission Lines*. John Wiley & Sons, 1994.

[18] D. Xiu and G. E. Karniadakis, "The Wiener-Askey polynomial chaos for stochastic differential equations," *SIAM J. Sci. Comput.*, vol. 24, no. 2, pp. 619–644, 2002.

[19] P. Manfredi, D. Vande Ginste, D. De Zutter, and F. G. Canavero, "Improved polynomial chaos discretization schemes to integrate interconnects into design environments," *IEEE Microwave and Wireless Components Letters*, vol. 23, no. 3, pp. 116–118, Mar. 2013.

[20] K. S. J. L. Volakis and B. C. Usner, *Frequency Domain Hybrid Finite Element Methods for Electromagnetics*, ser. Synthesis Lectures on Computational Eelectromagnetics. Morgan & Claypool Publishers, 2006.

[21] P. Manfredi, D. Vande Ginste, D. De Zutter, and F. G. Canavero, "On the passivity of polynomial chaos-based augmented models for stochastic circuits," *IEEE Trans. on Circuits and Systems I, In Press*.

[22] P. J. Davis and P. Rabinowitz, *Methods of Numerical Integration*, 2nd ed. Dover Publications, 2007.

[23] N. Nakhla, A. E. Ruehli, M. S. Nakhla, R. Achar, and C. Chen, "Waveform relaxation techniques for simulation of coupled interconnects with frequency-dependent parameters," *IEEE Trans. on Advanced Packaging*, vol. 30, no. 2, pp. 257–269, May 2007.

[24] R. C. Jaeger and T. N. Blalock, *Microelectronic Circuit Design*, 2nd ed. McGraw-Hill, 2004.

[25] A. Papoulis, *Probability, Random Variables, and Stochastic Processes*, 3rd ed. McGraw-Hill, 1991.

[26] M. A. Abramowitz and I. A. Stegun, *Handbook of mathematical functions*. New York: Dover Publications, Inc., 1970.

[27] S. Grivet-Talocia, I. S. Stievano, and F. G. Canavero, "Hybridization of FDTD and device behavioral-modeling techniques," *IEEE Trans. Electromagn. Compat.*, vol. 45, no. 1, pp. 31–42, Feb. 2003.

[28] J. Bäck, F. Nobile, L. Tamellini, and R. Tempone, "Stochastic spectral Galerkin and collocation methods for PDEs with random coefficients: A numerical comparison," in *Spectral and High Order Methods for Partial Differential Equations*, ser. Lecture Notes in Computational Science and Engineering, J. S. Hesthaven and E. M. Rønquist, Eds. Springer Berlin Heidelberg, 2011, vol. 76, pp. 43–62.